Article

Correlation Between the Myopic Retinal Deformation and Corneal Biomechanical Characteristics Measured With the Corvis ST Tonometry

Shotaro Asano[1], Ryo Asaoka[1], Takehiro Yamashita[2], Shuichiro Aoki[1,3], Masato Matsuura[1,4], Yuri Fujino[1,4], Hiroshi Murata[1], Shunsuke Nakakura[5], Yoshitaka Nakao[6], and Yoshiaki Kiuchi[6]

[1] Department of Ophthalmology, Graduate School of Medicine and Faculty of Medicine, The University of Tokyo, Tokyo, Japan
[2] Kagoshima University Graduate School of Medical and Dental Sciences, Kagoshima, Japan
[3] Department of Ophthalmology, Sapporo City General Hospital, Hokkaido, Japan
[4] Department of Ophthalmology, Graduate School of Medical Sciences, Kitasato University, Kanagawa, Japan
[5] Department of Ophthalmology, Saneikai Tsukazaki Hospital, Hyogo, Japan
[6] Department of Ophthalmology and Visual Science, Hiroshima University, Hiroshima, Japan

Purpose: We previously reported that the retinal deformation due to myopia was represented by the peripapillary retinal arteries angle (PRAA). In this study, we investigated the relationship between the PRAA and biomechanical properties measured with Corvis ST (CST) tonometry.

Methods: Thirty-four normative eyes of 34 subjects who underwent CST measurement were enrolled. The PRAA was calculated from a fundus photograph. Variables related to the PRAA were identified from age, axial length, spherical equivalent refractive error, and 10 CST parameters using model selection with the second-order bias-corrected Akaike information criterion index.

Results: The PRAA was best described with axial length (coefficient $= -5.66$, $P < 0.0001$), maximum deflection amplitude (mm; coefficient $= 130.5$, $P = 0.0004$), and deflection amplitude ratio (DA ratio) 2 mm (coefficient $= -25.8$, $P = 0.0032$), where mm was the amount of the maximum corneal apex movement and DA ratio 2 mm was the ratio between the deformation amplitudes at the apex and 2 mm away from the apex. The optimal model was significantly better than the model only with axial length ($P = 0.0014$, analysis of variance).

Conclusions: The PRAA was significantly better described with the CST parameters compared to the axial length model only; eyes with small PRAA (larger myopic retinal deformation) showed narrow and shallow maximum corneal deflection.

Translational Relevance: The Corvis ST parameters, which represents corneal biomechanical characteristics, were associated with myopic retinal deformation.

Introduction

Recently, myopia has been considered a major health issue,[1] because the global prevalence of myopia has increased rapidly in the past 50 years, especially in east and southeast Asia.[1–4] The Tajimi study has revealed that the incidence of myopia in the Japanese population was the highest in the world, with an incidence of 41.8% for myopia <-0.5 diopters (D)

and 5.5% for myopia <-6.0 D in individuals 40 years old.[5] Myopia also is considered to be related to various ophthalmologic diseases, such as cataract,[6] glaucoma,[7] choroidal neovascularization,[8] and retinal detachment.[9]

Myopia causes manifold ocular structural changes. For instance, a previous study indicated that the severity of myopia represented by longer axial length (AL) and more negative spherical equivalent refrac-

tive error (SERE) was related to the severity of myopic maculopathy.[10] In particular, previous studies showed that the retina was mechanically stretched around the papillomacular bundle in myopic eyes, and this retinal deformation was represented by the circumpapillary retinal nerve fiber layer (cpRNFL) peak angles and also peripapillary retinal arteries angle (PRAA).[11–13] Of note, the correlation between AL and the cpRNFL peak angle or PRAA was merely moderate ($r = -0.49$ or -0.38, respectively), which implies there is a wide variety in the magnitudes of retinal deformation even in eyes with an identical AL value.[11,14] However, the cpRNFL thickness can be affected by various ocular conditions, such as age[15] and glaucoma.[11] PRAA and cpRNFL peaks angle were very closely associated with the correlation coefficient value of 0.92 in young healthy subjects,[11] and PRAA is not affected by the aforementioned issues. Moreover, PRAA can be identified very easily in a fundus photograph. Hence, PRAA may be superior to cpRNFL peaks angle in the universal usefulness in estimating the retinal deformation due to myopia.

Recent development of Corvis ST (CST) tonometry has enabled us to evaluate the corneal biomechanical properties in detail, by capturing the sequential images of corneal movement following application of an air jet. We previously reported the association between myopic retinal deformation and corneal biomechanical properties measured with CST using the software version 1.00r30.[16] However, CST currently uses a newer software (version 1.13b1361), which yields a much larger number of raw parameters (previously 12 and currently 29 parameters). Moreover, the current CST software displays six summary parameters calculated from the 29 raw parameters, which enables us to analyze corneal elasticity and stiffness. This is very important clinically, because raw CST parameters merely show the shape of the cornea at each timing, in contrast to the newly available summary parameters.

We investigated the relationship between biomechanical properties and the myopic retinal deformation measured with PRAA using the newly introduced CST parameters.

Methods

Subjects

The study protocol was approved by the institutional review board of University of Tokyo Hospital, University of Hiroshima Hospital, and Tsukazaki Hospital, and adhered to the tenets of the Declaration of Helsinki. Informed consent was obtained from each subject.

Eyes undergoing CST measurements at the University of Tokyo Hospital, University of Hiroshima Hospital, or Tsukazaki Hospital between January 2016 and December 2017 were reviewed retrospectively, and 34 eyes of 34 subjects with no known eye diseases as determined by examining their medical histories were enrolled. Eligible criteria were: no pathologic findings as determined by slit-lamp microscopy, ophthalmoscopy, and/or optical coherence tomography (OCT); best-corrected visual acuity ≤0.1 logMAR units; SERE ≥−6 D; and intraocular pressure ≤21 mm Hg as measured using Goldmann applanation tonometry. Criteria for exclusion were known ocular diseases, such as glaucoma, staphyloma, and optic disc anomalies; systemic diseases, such as hypertension and diabetes; the presence of visual field (VF) defects; and/or a history of refractive or any intraocular surgery.

### Measurements of AL and Refractive Error

AL was measured using the optical biometer (OA-2000; Tomey, Nagoya, Japan) three times and an average value was calculated. Refractive error was measured with the Topcon KR8800 autorefractometer/keratometer (Topcon, Tokyo, Japan), and the SERE was calculated.

Peripapillary Retinal Arteries Angle (PRAA)

The identification of PRAA has been reported previously.[14] In short, optic disc color fundus photographs were obtained using either OCT (OCT-2000; Topcon) or a retinal camera (TRC-50DX; Topcon). ImageJ software (available in the public domain at https://imagej.nih.gov/ij/; National Institutes of Health, Bethesda, MD) was used to draw a 3.4-mm diameter peripapillary scan circle on the obtained fundus photographs. Then, PRAA was calculated from the points where the 3.4 mm-diameter peripapillary scan circle and the superotemporal/infratemporal major retinal arteries intersected (Fig. 1). Magnification effects of the camera were corrected using the Littmann's formula.[17]

CST Tonometry

As detailed previously,[18] CST monitors the corneal response to an air puff pulse during the inward and outward movements with a high-speed Scheimpflug
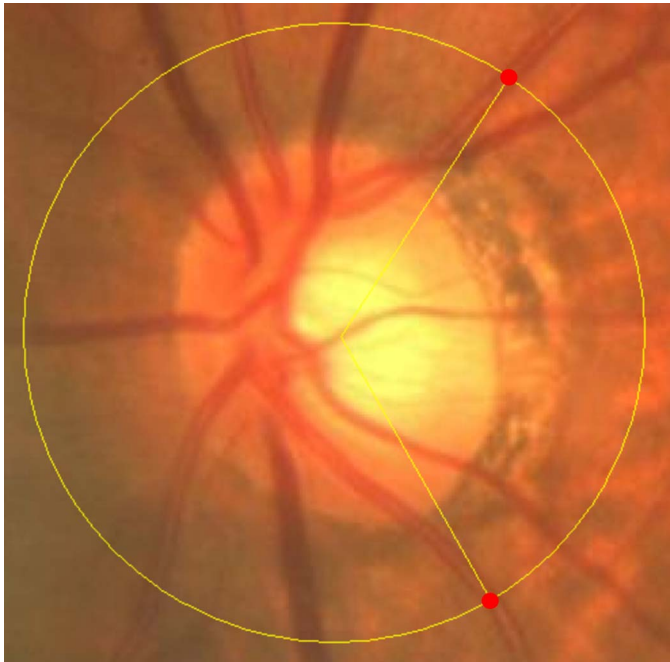
Figure 1. Measurement of PRAA (left eye). The PRAA was calculated from using the points where the 3.4-mm diameter peripapillary scan circle (*yellow*) and the superotemporal/infratemporal major retinal arteries intersected (*red dots*). The right eye was mirror-imaged.

camera, capturing 4330 frames per second. This imaging system allows us to investigate the dynamic inspection of the actual deformation process in vivo.[19] From the total of 36 corneal biomechanical properties measurable with the new version of CST, following our previous report, we used 10 summary CST parameters:[20]

- Ambrosio Relational Thickness horizontal (ARTh): The quotient and change of the corneal thickness.[21]
- Integrated Radius: The integrated area under the radius of the inversed curvature during the concave phase.[21]
- Stiffness parameter (SP-A1): The resulting pressure on the cornea divided by the deflection amplitude at the first applanation.[22]
- Corneal biomechanical index (CBI): The combination of the summary parameters indicating the likelihood of subclinical keratoconus and corneal ectasia.[21]
- Deflection amplitude ratio (DA ratio) 1 mm: The ratio of deflection amplitude (the corneal movement compensating the eye movement) at apex and at 1 or 2 mm.

- DA ratio 2 mm: The ratio of deflection amplitude (the corneal movement compensating the eye movement) at apex and at 2 mm.
- Whole eye movement (WEM; ms): The duration of the eye during the examination.
- WEM (mm): The total amount of the eye movement during the examination.
- Maximum Deflection amplitude (ms): The duration of the corneal movement compensating for WEM.
- Maximum Deflection amplitude (mm): The maximum amount of the corneal movement compensating for WEM.

CST (software version; ver. 1.13b1361) measurements were performed three times on the same day with at least a 5-minute interval between each measurement. Only reliable CST measurements, according to the 'OK' quality index displayed on the device monitor, were used.

Statistical Analysis

First, the relationships between PRAA and the 13 variables of age, AL, SERE, and the 10 CST parameters (WEM [mm], WEM [ms], Maximum deflection amplitude [mm], Maximum deflection amplitude [ms], DA ratio 1 mm, DA ratio 2 mm, ARTh, Integrated Radius, SP-A1, and CBI) were evaluated using the univariate linear regression analysis. The following relationship between these variables were calculated using the multivariate linear regression analysis, and finally the model selection was performed using the second-order bias-corrected Akaike information criterion (AICc) index; the optimal model for the PRAA was identified from the 2^{13} patterns using the 13 candidate variables. The Akaike information criterion index (AIC)[23] is defined as follows:

$$AIC = -2\ln L + 2K,$$

where L and K represent the maximized likelihood function and asymptotic bias correction term. The AICc is a corrected version of the AIC,[24] which provides an accurate estimation even when the sample size is small,[25] defined as follows:

$$AICc = AIC + \frac{2K(K+1)}{n-K-1},$$

where n stands for the sample size. The decrease in AICc indicates the improvement of the model.[26] The selected variables through the model selection were regarded as significant, because they provided us the

Table 1. Demographic Data of the Subjects

Variables	Value
Age, y, mean ± SD (range)	41.9 ± 17.8 (24–77)
Sex, male/female	18/16
Axial length, mm, mean ± SD (range)	24.6 ± 1.8 (21.5–28.1)
Spherical equivalent refractive error, D, mean ± SD (range)	−2.80 ± 4.4 (−10.3–4.00)
Keratometry, mm, mean ± SD (range)	8.00 ± 0.420 (7.36–9.08)
PRAA, degree, mean ± SD (range)	137 ± 14.8 (102–162)

objective measures for selecting among different models fitted to data considering the contributions and interactions between parameters.[27] The log-likelihood values of a paired model were compared using the analysis of variance (ANOVA) test.

All statistical analyses were performed using R (version 3.4.3, available in the public domain at http://www.R-project.org/).

Results

The demographics of the studied eyes are shown in Table 1. Table 2 shows the summary statistics of CST parameters.

The results of univariate linear regression between the PRAA and the 13 variables of age, AL, SERE, and the 10 CST parameters are shown in Table 3. The increase in AL and decrease in SERE were significantly related to the decrease in PRAA (coefficient = −4.33 with $P = 0.0015$, and coefficient = 1.61 with $P = 0.0046$, respectively).

The optimal linear model for the PRAA was identified as follows: PRAA = 265.5 − 5.66 (Standard Error [SE] = 1.14, $P < 0.0001$) × AL + 130.5 (SE = 32.8, $P = 0.0004$) × Maximum deflection amplitude [mm] − 25.8 (SE = 8.05, $P = 0.0032$) × DA ratio 2 mm

(AICc = 265.1). The log-likelihood of the optimal model was significantly larger than that of the model only with AL (AICc = 274.7, $P = 0.0014$, ANOVA).

Discussion

In the current study, we analyzed the relationship between myopic retinal deformation estimated by PRAA and corneal biomechanical properties represented by the new CST parameters, using 34 eyes of 34 healthy participants. As a result, PRAA was significantly better described with the CST parameters compared to the AL model only; eyes with small PRAA (larger myopic retinal deformation) exhibited narrow and shallow maximum corneal deflection.

As suggested by the optimal model for PRAA in our study, decreased maximum deflection amplitude (mm) and increased DA ratio 2 mm were associated with the larger myopic retinal deformation (smaller PRAA). Maximum deflection amplitude (mm) is the amount of the corneal apex movement compensating for the total eye movement during the examination, whereas DA ratio 2 mm is calculated by the ratio between the deformation amplitudes at the apex and at 2 mm away from the apex.[20] We recently investigated the relationship between circumpapillary

Table 2. Summary Statistics of Corvis ST Parameters

Variables	Mean ± Standard Deviation (Range)
Whole eye movement, mm	0.29 ± 0.08 (0.17–0.54)
Whole eye movement, ms	22.20 ± 0.91 (19.55–23.92)
Maximum deflection amplitude, mm	0.91 ± 0.07 (0.75–1.05)
Maximum deflection amplitude, ms	16.29 ± 0.70 (14.98–19.40)
DA ratio 1 mm	1.58 ± 0.04 (1.50–1.66)
DA ratio 2 mm	4.32 ± 0.32 (3.72–4.87)
ARTh	507.29 ± 123.35 (362.61–888.78)
Integrated radius	7.94 ± 0.87 (6.59–9.55)
SP-A1	100.25 ± 18.91 (70.05–169.29)
CBI	0.08 ± 0.14 (0–0.59)

Table 3. Results of Univariate Linear Regression Between PRAA and the Values of Age, Axial Length, Spherical Equivalent Refractive Error, and Ten CST Parameters

Variables	Coefficient	SE	P Value	AICc
Age, y	0.281	0.139	0.052	281.5
Axial length, mm	−4.33	1.25	0.0015*	274.7
Spherical equivalent refractive error, D	1.61	0.528	0.0046*	276.9
Whole eye movement, mm	80.9	28.0	0.0068*	277.7
Whole eye movement, ms	0.197	0.173	0.26	284.2
Maximum deflection amplitude, mm	70.6	33.2	0.041*	281.1
Maximum deflection amplitude, ms	0.113	0.176	0.53	285.1
DA ratio 1 mm	−27.1	62.4	0.67	285.4
DA ratio 2 mm	4.48	8.07	0.58	285.2
ARTh	0.00249	0.0212	0.91	285.5
Integrated radius	1.69	3.01	0.56	285.2
SP-A1	−0.219	0.133	0.11	282.8
CBI	26.3	17.8	0.15	283.3

* $P < 0.05$.

retinal nerve fiber layer (cpRNFL) peak angle and the older CST raw parameters (version 1.00r30) and cpRNFL peak angle was best described using AL and CST − measured A1 length, A1 time, and A2 time (cpRNFL peaks angle $= -901.1 + 132.7 \times$ A1 length $+ 27.8 \times$ A1 time $+ 31.0 \times$ A2 time $- 3.4 \times$ axial length).[16,28] The newer CST parameters were developed mainly to represent the elasticity and stiffness of the cornea. Our study suggested PRAA was better represented using the newer CST parameters of the magnitude of maximum deflection amplitude and DA ratio 2 mm, which enabled us to directly interpret the obtained results.

Miki et al.[29] examined the relationship between AL and CST maximum deflection amplitude, and suggested that greater maximum corneal deflection was observed in eyes with longer AL. They inferred this tendency was due to a low viscous damping property in eyes with longer AL, which agreed with the previous report that eyes with long AL had small corneal energy absorption.[16] However, of note, myopic retinal deformation cannot be fully explained only with AL and PRAA exceeded in its description, as we reported previously.[11] According to the current result, eyes with greater myopic retinal deformation (smaller PRAA) showed shallower maximum corneal deflection. The entire mechanism of this finding is unclear, but it may be because eyes with small PRAA suggest that retinal deformation is particularly large at the posterior pole of the eye and the shape of an eyeball is distorted. If enlargement of an eye occurs equally in the whole eye, PRAA would remain relatively large. This implies eyes with PRAA (and long AL) resist the deformation associated with the elongation of an eye, and such eyes may show shallow maximum corneal deflection. Furthermore, our results suggested that myopic retinal deformation was better analyzed using DA ratio 2 mm, in addition to maximum corneal deflection. As a result, it is suggested that large myopic retinal deformation is associated with long AL and small (narrow and shallow) maximum corneal deflection in the CST measurement.

There are a couple of limitations in our study. First, this study had a retrospective and cross-sectional nature. A further longitudinal study in a younger population in particular will enable us to better understand the relationship between myopic retinal deformation and corneal biomechanical properties. Second, a further validation of the derived optimal model is needed, preparing an independent validation dataset, which should be conducted in a future study. In addition, it would be further informative if corneal topographic data are analyzed, using Pentacam.

In conclusion, corneal biomechanical properties measured using the new CST summary parameters were associated with myopic retinal deformation. Eyes with small PRAA (larger myopic retinal deformation) had small (narrow and shallow) maximum corneal deflection.

Acknowledgments

References

1. Morgan IG, Ohno-Matsui K, Saw S-M. Myopia. *The Lancet*. 2012;379:1739–1748.
2. Morgan I, Rose K. How genetic is school myopia? *Prog Retin Eye Res*. 2005;24:1–38.
3. Pan CW, Ramamurthy D, Saw SM. Worldwide prevalence and risk factors for myopia. *Ophthalmic Physiol Opt*. 2012;32:3–16.
4. Lin LL-K, Shih Y-F, Hsiao CK, Chen C. Prevalence of myopia in Taiwanese schoolchildren: 1983 to 2000. *Ann Acad Med Singapore*. 2004;33:27–33.
5. Sawada A, Tomidokoro A, Araie M, Iwase A, Yamamoto T, Group TS. Refractive errors in an elderly Japanese population: the Tajimi study. *Ophthalmology*. 2008;115:363–370. e363.
6. Lim R, Mitchell P, Cumming RG. Refractive associations with cataract: the blue mountains eye study. *Invest Ophthalmol Vis Sci*. 1999;40:3021–3026.
7. Mitchell P, Hourihan F, Sandbach J, Wang JJ. The relationship between glaucoma and myopia: the Blue Mountains Eye Study. *Ophthalmology*. 1999;106:2010–2015.
8. Ohsugi H, Ikuno Y, Shoujou T, Oshima K, Ohsugi E, Tabuchi H. Axial length changes in highly myopic eyes and influence of myopic macular complications in Japanese adults. *PLoS One*. 2017;12:e0180851.
9. Fang X, Weng Y, Xu S, et al. Optical coherence tomographic characteristics and surgical outcome of eyes with myopic foveoschisis. *Eye (Lond)*. 2009;23:1336.
10. Zhao X, Ding X, Lyu C, et al. Morphological characteristics and visual acuity of highly myopic eyes with different severities of myopic maculopathy [published online ahead of print, December 18, 2018).
11. Yamashita T, Asaoka R, Tanaka M, et al. Relationship between position of peak retinal nerve fiber layer thickness and retinal arteries on sectoral retinal nerve fiber layer thickness. *Invest Ophthalmol Vis Sci*. 2013;54:5481–5488.
12. Yoo YC, Lee CM, Park JH. Changes in peripapillary retinal nerve fiber layer distribution by axial length. *Optom Vis Sci*. 2012;89:4–11.
13. Hong SW, Ahn MD, Kang SH, Im SK. Analysis of peripapillary retinal nerve fiber distribution in normal young adults. *Invest Ophthalmol Vis Sci*. 2010;51:3515–3523.
14. Asano S, Asaoka R, Yamashita T, et al. Relationship between the shift of the retinal artery associated with myopia and ocular response analyzer waveform parameters. *Transl Vis Sci Technol*. 2019;8:15.
15. Lee MW, Kim JM, Shin YI, Jo YJ, Kim JY. Longitudinal changes in peripapillary retinal nerve fiber layer thickness in high myopia: a prospective, observational study. *Ophthalmology*. 2018;126:522–528.
16. Matsuura M, Murata H, Nakakura S, et al. The relationship between retinal nerve fibre layer thickness profiles and CorvisST tonometry measured biomechanical properties in young healthy subjects. *Sci Rep*. 2017;7:414.
17. Littmann H. Zur Bestimmung der wahren Größe eines Objektes auf dem Hintergrund des lebenden Auges. *Klin Monbl Augenheilkd*. 1982;180:286–289.
18. Hong J, Xu J, Wei A, et al. A new tonometer–the Corvis ST tonometer: clinical comparison with noncontact and Goldmann applanation tonometers. *Invest Ophthalmol Vis Sci*. 2013;54:659–665.
19. Ambrósio R Jr, Ramos I, Luz A, et al. Dynamic ultra high speed Scheimpflug imaging for assessing corneal biomechanical properties. *Rev Bras Oftalmol*. 2013;72:99–102.
20. Roberts CJ, Mahmoud AM, Bons JP, et al. Introduction of two novel stiffness parameters and interpretation of air puff–induced biomechanical deformation parameters with a dynamic Scheimpflug analyzer. *J Refract Surg*. 2017;33:266–273.
21. Vinciguerra R, Ambrosio R Jr, Elsheikh A, et al. Detection of keratoconus with a new biomechanical index. *J Refract Surg*. 2016;32:803–810.
22. Mercer RN, Waring GO IIII, Roberts CJ, et al. Comparison of corneal deformation parameters in keratoconic and normal eyes using a noncontact tonometer with a dynamic ultra-high-speed Scheimpflug camera. *J Refract Surg*. 2017;33:625–631.

23. Akaike H. Information theory and an extension of the maximum likelihood principle. In: Petrov BN, Czaki F, eds. *Proceedings of the 2nd International Symposium on Information*. Budapest: Akademiai Kiado; 1973:267–281.

24. Sugiura N. Further analysts of the data by Akaike's information criterion and the finite corrections: Further analysts of the data by Akaike's. *Commun Stat Theory Methods*. 1978; 7:13–26.

25. Burnham KP, Anderson DR. Multimodel inference. *Sociol Methods Res*. 2016;33:261–304.

26. Mallows CL. Some comments on C p. *Technometrics*. 1973;15:661–675.

27. Johnson DH. The Insignificance of statistical significance testing. *J Wildl Manage*. 1999;63: 763–772.

28. Matsuura M, Hirasawa K, Murata H, et al. The relationship between Corvis ST tonometry and ocular response analyzer measurements in eyes with glaucoma. *PLoS One*. 2016;11:e0161742.

29. Miki A, Maeda N, Ikuno Y, Asai T, Hara C, Nishida K. Factors associated with corneal deformation responses measured with a dynamic Scheimpflug analyzer. *Invest Ophthalmol Vis Sci*. 2017;58:538–544.